Magnetospheric Chorus: Amplitude and Growth Rate

W. J. BURTIS AND R. A. HELLIWELL

Radioscience Laboratory, Stanford University, Stanford, California 94305

A new study of the amplitude of magnetospheric chorus using 1966–1967 data from the Stanford University/Stanford Research Institute VLF receivers on Ogo 1 and Ogo 3 has provided the following results: (1) The band-limited character of magnetospheric chorus in general and the double-banding of near-equatorial chorus were confirmed. Activity at frequencies outside the chorus band was usually below the noise level of the VLF receiver, often more than 40 dB below peak chorus amplitudes. (2) Peak intensities typically ranged from 1 to 100 pT (mγ); power spectral densities from 10^{-28} to 10^{-22} T^2/Hz were observed. (3) Chorus amplitude tended to be inversely correlated with frequency, implying lower intensities at lower L values. (4) Individual chorus emissions often showed a characteristic amplitude variation, with rise times of 10 to 300 ms, a short duration at peak amplitude, and decay times of 100 to 3000 ms. (5) Growth was often approximately exponential, with rates from 200 to nearly 2000 dB/s. (6) Rate of change of frequency was found in many cases to be independent of emission amplitude, in agreement with the cyclotron feedback theory of chorus (Helliwell, 1967, 1970). (7) In spite of the relatively high sensitivity of the magnetic detectors employed in these observations, a major part of the electromagnetic spectrum at VLF in the outer magnetosphere was below the instrumental noise level; further space observations at VLF using magnetic detectors of greatly increased sensitivity are therefore desirable.

INTRODUCTION

Previous satellite studies of VLF chorus have provided typical values for peak amplitudes in the upper ionosphere [*Taylor and Gurnett*, 1968] and at high altitudes in the magnetosphere [*Dunckel and Helliwell*, 1969; *Tsurutani and Smith*, 1974]. *Dunckel and Helliwell* [1969] measured the power spectrum of VLF noise in the magnetosphere, but the observations were made during a geomagnetically quiet period with relatively little chorus activity. *Tsurutani and Smith* [1974] showed an average power spectrum for one 8-min period of active chorus. The present study extends these measurements of power spectra to representative examples of band-limited magnetospheric chorus and reports on the first measurements of the time variations of the amplitudes of individual elements, or discrete emissions, within the chorus band. Two important new results are obtained: (1) growth is often exponential in time, with growth rates ranging from about 200 to 2000 dB/s, and (2) the time rate of change of frequency is essentially independent of changes in emission amplitude.

This report, based on a moderate quantity of representative data, supplements a comprehensive statistical survey providing information on the occurrence and normalized frequency of magnetospheric chorus [*Burtis and Helliwell*, 1975]. Two sources of amplitude information were used in the present study. The first was digital data from the Stanford University/Stanford Research Institute VLF sweeping receivers on board Ogo 3. The band 1 receiver covers the range 0.2–1.6 kHz in 256 steps with a 3-dB bandwidth of 40 Hz; the band 2 receiver covers the range 1.6–12.5 kHz in 256 steps with a 3-dB bandwidth of 160 Hz; the band 3 receiver covers higher frequencies, at which chorus was not observed. The sweep rate for each receiver is 2.3, 18.4, or 147 s/sweep depending on the bit rate of the pulse count modulation telemetry. Instrumentation details are given by *Ficklin et al.* [1967]. The second source of amplitude information was the Stanford University/Stanford Research Institute broad band VLF receiver amplitude VCO on Ogo 1 (the voltage controlled oscillator is used for a different purpose on Ogo 3). The VCO frequency deviation is quasi-logarithmically related to the broad band (0.3–12.5 kHz) amplitude, and the response time is ~3 ms [*Ficklin et al.*, 1967]. Unfortunately the calibration of the VCO is somewhat uncertain, since its frequency drifted with spacecraft temperature after launch. However, by using an internal 1-kHz sawtooth calibration signal as reference, chorus intensities are found to be comparable to those measured with the sweeping receivers and are believed to be accurate to within ±6 dB. The threshold sensitivity of both the Ogo 1 and the Ogo 3 receiver varies from 0.003 pT (mγ) at 12.5 kHz to 0.24 pT at 0.2 kHz; the dynamic range is 90 dB.

POWER SPECTRUM

Six representative examples of chorus observed with the sweeping receivers are shown in Figure 1. Parts *a*, *b*, and *c* (on the left) each show a single sweep on the band 1 receiver, while parts *d*, *e*, and *f* (on the right) each show a single sweep of the band 2 receiver. In all cases, activity at frequencies other than the band shown is near or below noise level. Universal time at the start of the sweep is shown to the nearest second above each panel. All examples are at high bit rate (2.3 s/sweep), except panels *a* and *f*, which are at low bit rate (147 s/sweep).

Amplitudes measured with the magnetic antenna are indicated in dBpT, i.e., decibels above 1 pT (1 pT = 1 mγ = 10^{-12} W/m^2). The 3-dB bandwidths of the band 1 and band 2 sweeping receiver filters are 40 and 160 Hz, respectively. Thus an amplitude of 20 dBpT (10 pT) corresponds to a power spectral density of 2.5 × 10^{-24} T^2/Hz in band 1 and 0.625 × 10^{-24} T^2/Hz in band 2. The indicated amplitude calibration is strictly correct only at the frequency of 1 kHz in band 1 and 10 kHz in band 2. For higher (lower) frequencies the indicated amplitudes must be decreased (increased) ~6 dB/octave to correct for the increased sensitivity of the VLF receiver at higher frequencies.

Since chorus is composed of discrete elements with durations less than the sweep period, the spectrum changes markedly from one sweep to the next. The spectrum may show multiple spikes if the sweep passes through several discrete emissions, or it may show a broad band of activity if the chorus is accompanied by hiss. In general, the sweeping receiver data confirm the band-limited nature of magnetospheric chorus [*Burtis and Helliwell*, 1969] and the double

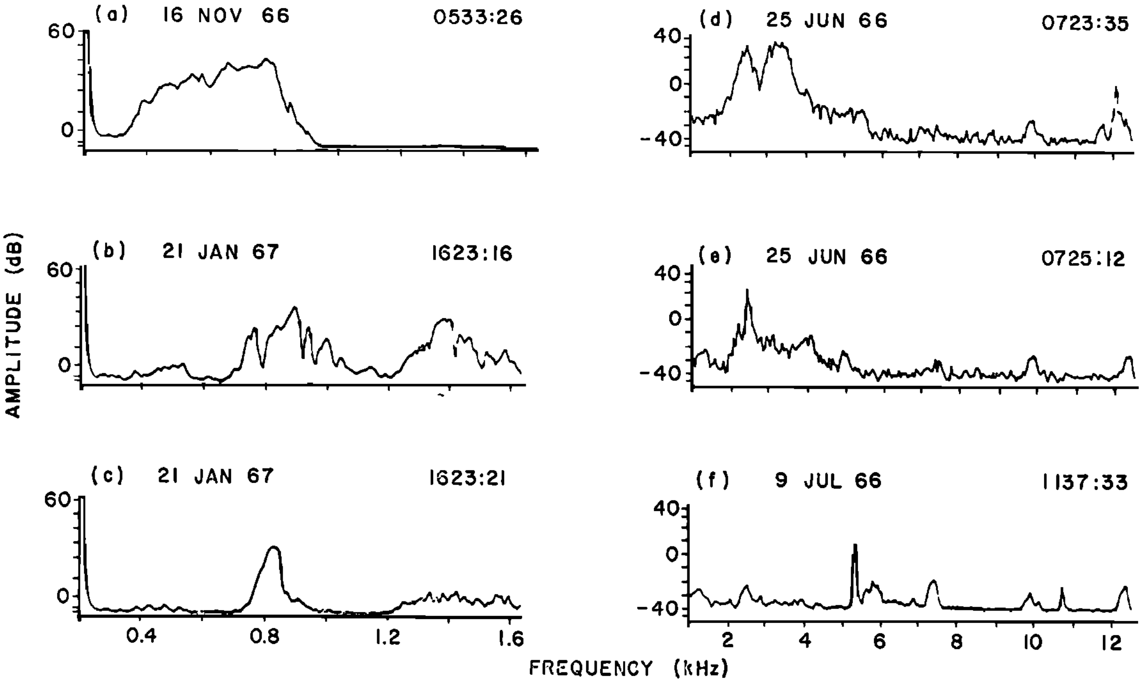

Fig. 1. Representative amplitude spectra of magnetospheric chorus. Parts *a*, *b*, and *c* (left) each show a single sweep of the band 1 receiver; parts *d*, *e*, and *f* (right) each show a single sweep of the band 2 receiver. Amplitudes are in decibels above 1 pT (1 pT = 1 mγ = 10^{-12} W/m^2), except parts *b* and *c* (electric antenna) are in decibels above 10 μV/m. Each spectrum is discussed in detail in the text.

banding of chorus observed near the dipole equator [*Burtis and Helliwell*, 1971, 1975].

One of the strongest emissions observed in the present study is illustrated in Figure 1*a*. Ogo 3 was outbound in the noon quadrant, L = 11.7, dipole latitude λ = 20°. Chorus was seen on the band 1 sweeping receiver from L = 10 to L = 12.5; observation of chorus at these unusually large L values is not unreasonable considering the low geomagnetic activity level (Kp = 1). The peak amplitude on this sweep is 140 pT at 0.8 kHz. Above the peak the amplitude drops 60 dB in less than 200 Hz. Although no broad band data are available for this time period, the relatively smooth trace over the 400-Hz range from 0.4 to 0.8 kHz suggests that the receiver is sweeping through a diffuse emission. Preceding and succeeding sweeps are 10–40 dB lower in amplitude and most have a narrower bandwidth, ~200 to 300 Hz.

A good example of a double chorus band seen near the equator is shown in Figure 1*b*. Ogo 3 was at L = 7.3, λ = −2°, LT = 1000; geomagnetic activity was moderate. The antenna was in the electric mode, so in this example the calibration scale is in decibels above 10 μV/m rather than in decibels above 1 pT. Peak amplitude in the lower band is 350 μV/m (at 0.88 kHz) and in the upper band is 180 μV/m (at 1.38 kHz). If one assumes a whistler mode refractive index of 10, these peaks correspond to wave B fields of 11 and 6 pT, respectively. Amplitudes at frequencies between the bands are some 30–40 dB below peak. The measured value of one half the local electron gyrofrequency $f_H/2$ is 1.23 kHz, i.e., near the lower edge of the upper band.

Figure 1*c* shows the second sweep following that of Figure 1*b*. In this case, broad band data show that the receiver was sweeping through a single emission in the lower band (peak amplitude 200 μV/m), while the upper band was diffuse and weak (13 μV/m). Because of the small angle between the frequency sweep (0.6 kHz/s) and the rising emission (1.2 kHz/s), the apparent 10-dB bandwidth of the emission, ~55 Hz, should be interpreted as an upper limit; the actual bandwidth may be much smaller. Any activity between the two bands is in this case below the noise level of the receiver (<1 μV/m).

An exceptionally strong emission observed with the band 2 receiver is shown in Figure 1*d*. Ogo 3 was at L = 4.6, λ = 6°, LT = 0050; geomagnetic activity is moderate (Kp = 3). The measured value of $f_H/2$ was 3.8 kHz, so the strongest activity (peak amplitude 180 pT) is below $f_H/2$. (The peak near 12 kHz is believed to be an intermodulation product of the lower frequency chorus activity with a local oscillator; the smaller peak near 10 kHz is the fourth harmonic of a satellite inverter.)

A very discrete 50-pT emission observed some 2 min later on the same pass is shown in Figure 1*e*. Satellite coordinates and f_H are nearly the same as those for Figure 1*d*. From the broad band spectrum it appears that the receiver is sweeping through a short falling tone at this frequency. Since the receiver sweep and the falling emission have opposite df/dt, the receiver pass band sweeps quickly across the emission. The apparent 20-dB emission bandwidth is 180 Hz (the nominal 3-dB bandwidth for band 2 is 160 Hz). Note inverter harmonics near 5, 7.5, 10, and 12.5 kHz.

Another very narrow band emission seen on a different pass is shown in Figure 1*f*. Ogo 3 was at L = 4.0, λ = −11°, LT = 0020; geomagnetic conditions were disturbed. Measured $f_H/2$ was 7.1 kHz. The peak emission amplitude is 4.5 pT, and the apparent 20-dB bandwidth is 160 Hz. The amplitude increases some 40 dB, from noise level to peak, in less than 200 Hz.

The peak narrow band amplitude of chorus emissions ranged from below the noise level to about 100 pT (~10^{-28} to ~10^{-22} T^2/Hz). Broad band intensities, obtained by integrating the power spectra, were several times the peak narrow band intensities. Peak broad band intensities measured by the Ogo 1 VCO ranged mainly from 1 to 200 pT. These chorus amplitudes are comparable to those found in previous satellite studies [*Taylor and Gurnett*, 1968; *Dunckel and Helliwell*, 1969; *Tsurutani and Smith*, 1974].

A general inverse correlation of amplitude with frequency was observed, although exceptions to this general relationship were not uncommon. The strongest peaks in the sweeping receiver data for a single Ogo 3 pass are indicated by the circled points in Figure 2. The points at the lowest frequencies, ~0.5 kHz, were observed near dipole $L = 6$; as the satellite traveled inbound in the midnight equatorial region over the next 45 min, the chorus frequency gradually increased to ~5 kHz near $L = 4$. Thus time is approximately related to frequency, and the temporal spacing between points is ~20 s (the absence of frequencies near 1.5 kHz is caused by a 10-min data gap). The range of amplitudes observed is even greater than that shown, since only the strongest peaks (about one of every 10 sweeps of the digital receiver) are plotted. Some of this amplitude variation is caused by the fact that the receiver does not in general sweep across the strongest portion of an emission, and some is caused by actual intensity variations from one emission to the next. The latter may be caused both by variations in source amplitude and by variations in propagation loss (weaker emissions may have propagated from a source off the field line of the satellite). With the exception of frequencies from 2 to 3 kHz, perhaps a local region or short period of unusually high resonant electron flux, there appears to be a slight overall decrease in amplitude with frequency.

Peak broad band amplitudes of chorus on six Ogo 1 passes in autumn 1966 are shown by the squares in Figure 2. Each point represents the strongest emission observed over a period of several minutes, while the error bars indicate the estimated ±6-dB uncertainty in the calibration of the Ogo 1 amplitude VCO. The average trend is toward lower amplitudes at higher frequencies, and the longest individual passes show the same trend. For example, over a 70-min period during the outbound local morning Ogo 1 pass of November 30, 1966, the peak amplitude increased from 3 pT at 6 kHz ($L = 4.1$, $\lambda = 10°$) to 22 pT at 0.6 kHz ($L = 7.7$, $\lambda = 38°$). Note that the variation of dipole latitude λ is in the wrong sense to account for the amplitude variation in terms of attenuation during propagation away from the equatorial source region.

Since chorus frequency tends to vary as L^{-3} [*Burtis and Helliwell,* 1969], Figure 2 implies decreasing chorus amplitude at lower L values. This may be related to the fact that the fluxes of 1- to 20-keV electrons decrease as the observing point moves inward toward the plasmapause [*Schield and Frank,* 1970]; the cyclotron interaction model proposed by *Helliwell and Crystal* [1973] predicts a positive correlation between emission amplitude and flux density of resonant electrons. It may be noted that the observed variation of amplitude with L is in the opposite direction from that predicted by *Kennel and Petschek* [1966]. They considered steady hiss far below the gyrofrequency rather than discrete emissions near half the gyrofrequency.

GROWTH RATE

The amplitude variations of individual chorus emissions were readily measured with the Ogo 1 broad band amplitude VCO, whose response time was ~3 ms. Typically, emissions were found to grow rapidly (rise time ~10–300 ms) to a peak amplitude of short duration and then to decay more slowly (decay time ~100–3000 ms). Growth and decay were often approximately exponential; however, it was not unusual for amplitude variations to be more complex.

Two typical examples of the amplitude variations of chorus emissions are shown in Figure 3. In both parts *a* and *b* the VLF spectrum from 5 to 10 kHz is shown in the upper half, while the amplitude VCO has been translated in frequency and inserted in the lower half. An amplitude scale, in dB above 1 pT, is shown on the right. The records, made with the Rayspan analyzer, have frequency resolution df = 64 Hz and time

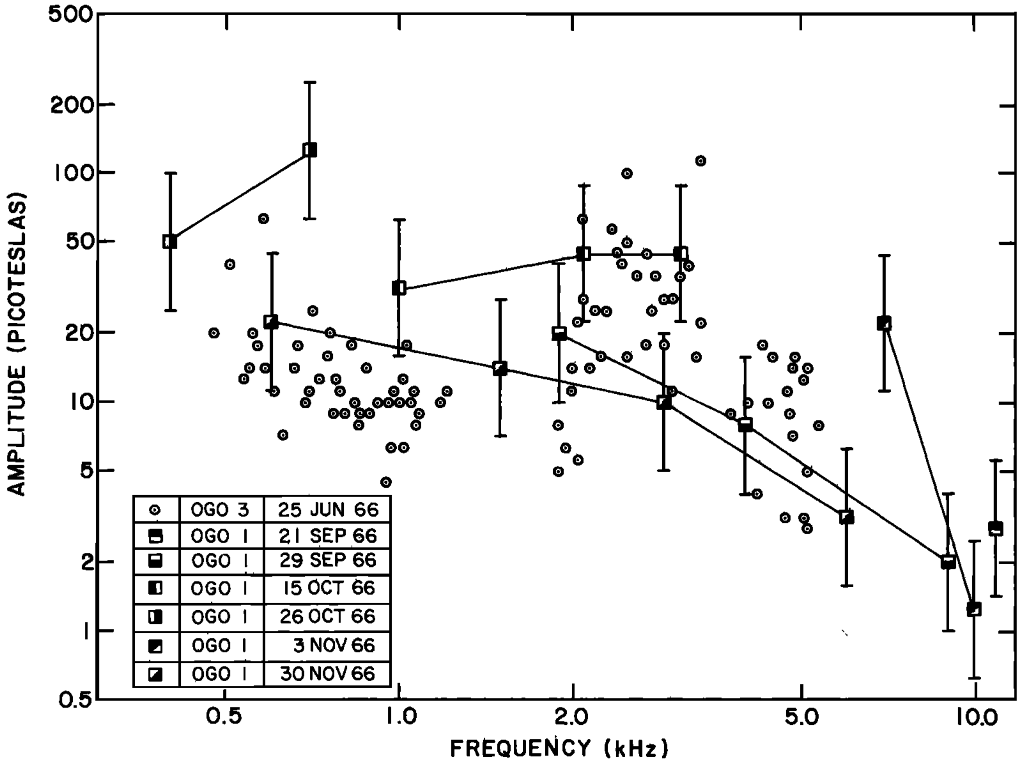

Fig. 2. Variation of peak amplitude with frequency. Circled points show the strongest narrow band (sweeping receiver) amplitudes for the Ogo 3 pass of June 25, 1966. Squares show peak broad band (VCO) amplitudes for six Ogo 1 passes in autumn 1966. Error bars indicate ±6-dB uncertainty in VCO calibration.

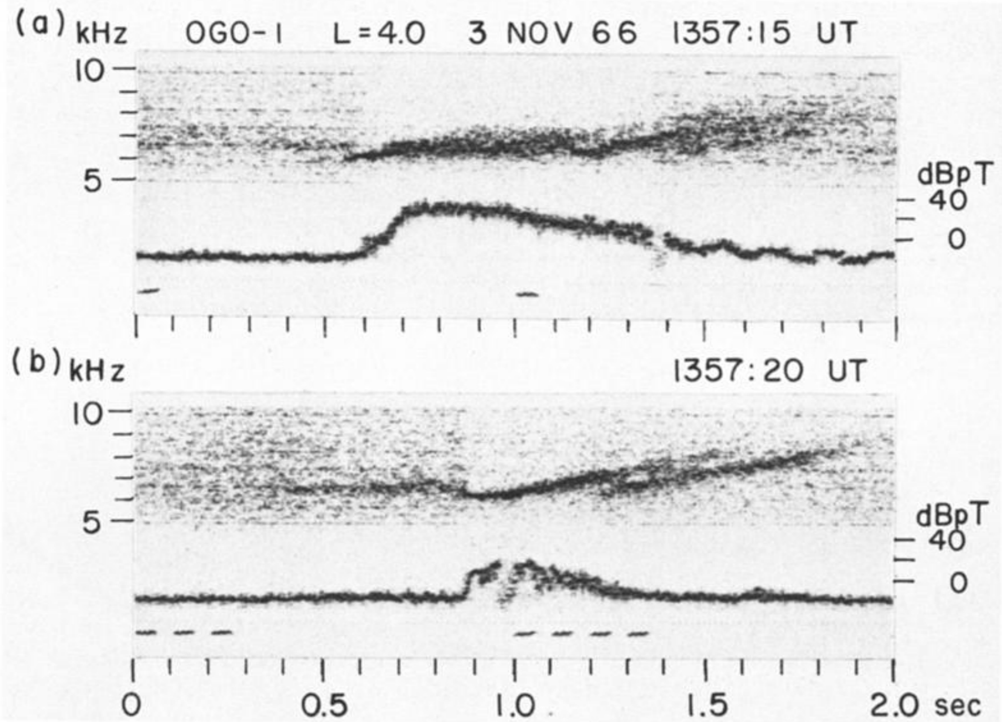

Fig. 3. Typical amplitude variations. In both parts *a* and *b* the VLF spectrum from 5 to 10 kHz is shown in the upper half, while the amplitude VCO has been inserted in the lower half. Note characteristic fast rise/slow decay amplitude variation.

resolution dt = 16 ms. The time scale has been expanded to show amplitude variations; a time code appears at the bottom of the records. The satellite was at $\lambda = 12°$, $L = 4.0$ near the dawn meridian. Geomagnetic activity was moderate; Kp varied between 2 and 5 during the preceding 48 hours. Chorus, consisting primarily of rising emissions, was observed for several hours on this pass.

A strong, isolated rising emission is shown in Figure 3*a*. The emission appears to arise spontaneously from the background noise; initially the bandwidth is small, but later it increases, and this emission appears to trigger a second, weaker emission at ~1.1 s. Weak constant frequency lines throughout the spectrum are attributed to unbalanced Rayspan filters and (after 1.4 s) to an internal calibration signal at 1 kHz and harmonics. (Note the automatic gain control attenuation of background noise caused by the strong emission.) The amplitude VCO in the lower half of part *a* shows a typical fast rise/slow decay intensity variation during the chorus emission. Prior to the emission the VCO is at the noise level (~0.14 pT at the chorus frequency of 6.5 kHz). During the growth phase of the emission the VCO frequency increases in a nearly linear manner, indicating exponential growth. The peak amplitude is 28 pT, some 46 dB above noise level, and the growth rate is 350 dB/s. The intensity then decreases gradually over a time span of about a second. Just before 1.4 s the VCO briefly drops off scale due to a sync pulse, while after 1.4 s the VCO shows a square wave due to the periodic internal calibration signal.

A weaker emission with a higher growth rate is shown in Figure 3*b*. This emission appears to begin with a small hook and is perhaps triggered by the weak narrow band hiss preceding the emission. Again the emission seems to trigger a second, weaker emission at 1.2 s. The amplitude VCO shows a very fast and nearly linear rise from the noise level to just below the peak intensity of 3.5 pT; the approximately exponential growth rate is 1120 dB/s. Near the amplitude peak (~1.0 s) the VCO briefly drops off scale due to a sync pulse. The emission amplitude then slowly decays to below noise level.

Narrow band emissions with complex amplitude variations are illustrated in Figure 4. In both parts *a* and *b* the VLF spectrum from 0 to 4 kHz is shown in the lower half, while the amplitude VCO has been inserted in the upper half. These Rayspan records again have resolution df = 64 Hz and dt = 16 ms. Interference lines from satellite inverters appear at 0.8 and 2.5 kHz. Ogo 1 was at $L = 5.3$, $\lambda = 24°$, LT = 1040; geomagnetic activity was moderately low ($Kp = 2$). These particular emissions were selected for analysis because they are discrete and well isolated from other emissions and hiss (approximately 16% of magnetospheric chorus includes falling tones, although rising tones are usually predominant [*Burtis*, 1974]).

In Figure 4*a*, two adjacent falling tones are shown, the first arising spontaneously at ~0.33 s and the second beginning at ~0.56 s. Other records made with expanded frequency scale show that the second falling tone begins at a frequency well separated from the tail of the first, so the second emission does not appear to be triggered by the first. During the first emission the amplitude rises, goes through a sharp null, and then rises again to a peak of 14 pT. The noise level at the chorus frequency of 1.9 kHz is ~0.45 pT. The average growth rate for this first emission is 270 dB/s, while the growth rate after the null is 730 dB/s. Note that there is little discontinuity in the spectral shape as the amplitude passes through the null. The second emission grows at an average rate of 180 dB/s to a peak amplitude of 6.3 pT and then decays at about the same rate.

A single pure falling tone with complex amplitude variations is shown in Figure 4*b*. The intensity rises slowly for ~80 ms, grows rapidly at a rate of 1030 dB/s to 16 pT, gradually decays, goes through a sharp null, rises again at ~490 dB/s to a peak of 22 pT, and finally decreases erratically to the noise level. The rate of frequency change of the emission is not markedly influenced by these amplitude fluctuations. Such

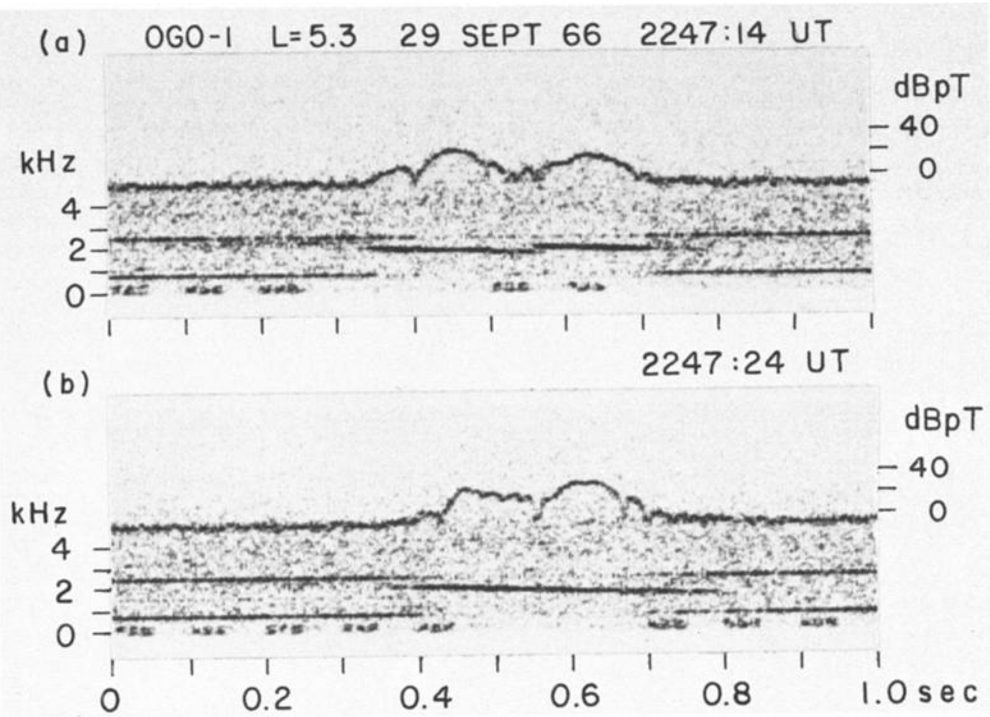

Fig. 4. Complex amplitude variation. In both parts *a* and *b* the VLF spectrum from 0 to 4 kHz is shown in the lower half, while the amplitude VCO has been inserted in the upper half. Note irregular amplitude variations seemingly unrelated to spectral shape of emissions.

complex variations in amplitude are definitely less common than the fast rise/slow decay response illustrated in Figure 3; however, not enough data have been studied to say whether such variations are typical of falling tones.

Average growth rates were measured for all isolated emissions appearing during the 2 min preceding and following the events shown in Figures 3 and 4. Growth rates ranged from ~200 to nearly 2000 dB/s, while intensities varied from ~1 to 30 pT. There appeared to be only a slight positive correlation between peak amplitude and growth rate during these two brief periods. Additional data must be analyzed to determine whether such a correlation exists over the longer term.

Growth rates of chorus emissions triggered by the VLF transmitter at Siple station, Antarctica, have been found to vary between 30 and 200 dB/s [*Helliwell,* 1974; *Helliwell and Katsufrakis,* 1974; *Stiles,* 1974]. Emissions artificially stimulated by NAA and Omega transmissions also show growth rates in the same range [*Stiles,* 1974]. The significantly higher growth rates of magnetospheric chorus observed by Ogo 1 may be related to the spontaneous nature of most chorus in the outer magnetosphere. Whistlers and man-made signals were never observed in the present study when the satellites were significantly beyond the plasmapause. Absence of such artificial triggering stimuli may allow the flux of resonant electrons to increase until emissions are spontaneously set off by the background noise in the magnetosphere. The higher resonant electron flux may then result in faster growth of emissions once they begin [*Helliwell and Crystal,* 1973].

A new and significant result, we believe, is the observation that the frequency rate of change of emissions is often essentially independent of relatively large amplitude variations (see Figures 3 and 4). This result supports the cyclotron feedback theory of *Helliwell* [1967, 1970], which predicts that the rate of change of frequency with time depends on the inhomogeneity of the medium and not on the amplitude of the growing wave.

Although the VLF receivers on Ogo 1 and Ogo 3 were among the most sensitive magnetic detectors yet flown, it is apparent that most of the electromagnetic spectrum at VLF in the outer magnetosphere was still below receiver threshold. Chorus, the predominant wave activity in the trough region ($4 \lesssim L \lesssim 10$), was detected only 27% of the time overall (occurrence was much higher under certain conditions) [*Burtis,* 1974; *Burtis and Helliwell,* 1975]. Even during periods of active chorus, radiation at frequencies outside the chorus band or during intervals between emissions was generally below the noise level of the receiver (see Figures 1, 3, and 4). It is interesting to speculate about the unknown lower amplitude VLF radiation. Very weak whistlers (dispersed spherics) or man-made signals (transmitters or power line harmonics) might be found to influence the onset time and/or frequency of chorus emissions, although such triggering signals have not been observed significantly beyond the plasmapause with present receiver sensitivities. Attenuated echoes of emissions that have been magnetospherically reflected near the LHR might provide a quantitative measurement of Landau damping. Weak resonances and even diffuse incoherent radiation might provide new information about the particle populations. And as is always the case in terra incognita, there is the possibility of discovering new geophysically significant phenomena. We suggest that serious consideration be given to the design of a VLF experiment with sufficient sensitivity to reach the lowest levels of background radiation of the outer magnetosphere.

Acknowledgments. The research work for this paper was supported by the National Aeronautics and Space Administration under grant NGL 05-020-008.

The Editor thanks R. E. Barrington for his assistance in evaluating this report.

REFERENCES

Burtis, W. J., Magnetospheric chorus, *Tech. Rep. SEL 74-041,* Radioscience Lab., Stanford Electron. Lab., Stanford Univ., Stanford, Calif., 1974.

Burtis, W. J., and R. A. Helliwell, Banded chorus—A new type of VLF radiation observed in the magnetosphere by Ogo 1 and Ogo 3, *J. Geophys. Res.*, *74*, 3002, 1969.
Burtis, W. J., and R. A. Helliwell, Normalized frequency of VLF banded chorus near the equator (abstract), *Eos Trans. AGU*, *52*, 332, 1971.
Burtis, W. J., and R. A. Helliwell, Magnetospheric chorus: Occurrence patterns and normalized frequency, submitted to *J. Geophys. Res.*, 1975.
Dunckel, N., and R. A. Helliwell, Whistler mode emissions on the Ogo 1 satellite, *J. Geophys. Res.*, *74*, 6371, 1969.
Ficklin, B. P., R. H. Stehle, C. Barnes, and M. E. Mills, The instrumentation for the Stanford University/Stanford Research Institute VLF experiment (B-17) on the Ogo 3 satellite, supplemental report, Stanford Res. Inst., Menlo Park, Calif., 1967.
Helliwell, R. A., A theory of discrete VLF emissions from the magnetosphere, *J. Geophys. Res.*, *72*, 4773, 1967.
Helliwell, R. A., Intensity of discrete VLF emissions, in *Particles and Fields in the Magnetosphere*, edited by B. McCormac, pp. 292–301, D. Reidel, Dordrecht, Netherlands, 1970.
Helliwell, R. A., Controlled VLF wave injection experiments in the magnetosphere, *Space Sci. Rev.*, *15*, 781, 1974.
Helliwell, R. A., and T. L. Crystal, A feedback model of cyclotron interaction between whistler mode waves and energetic electrons in the magnetosphere, *J. Geophys. Res.*, *78*, 7357, 1973.
Helliwell, R. A., and J. P. Katsufrakis, VLF wave injection into the magnetosphere from Siple station, Antarctica, *J. Geophys. Res.*, *79*, 2511, 1974.
Kennel, C. F., and H. E. Petschek, Limit on stably trapped particle fluxes, *J. Geophys. Res.*, *71*, 1, 1966.
Schield, M. A., and L. A. Frank, Electron observations between the inner edge of the plasma sheet and the plasmasphere, *J. Geophys. Res.*, *75*, 5401, 1970.
Stiles, G. S., Digital spectra of artificially stimulated VLF emissions, *Tech. Rep. SEL 74-049*, Radioscience Lab., Stanford Electron. Lab., Stanford Univ., Stanford, Calif., 1974.
Taylor, W. W. L., and D. A. Gurnett, Morphology of VLF emissions observed with the Injun 3 satellite, *J. Geophys. Res.*, *73*, 5615, 1968.
Tsurutani, B. T., and E. J. Smith, Postmidnight chorus: A substorm phenomenon, *J. Geophys. Res.*, *79*, 118, 1974.

(Received November 13, 1974;
revised February 10, 1975;
accepted February 25, 1975.)